



Northward shift of boreal tree cover confirmed by satellite record

Authors

Min Feng^{1,2}; Joseph O. Sexton¹; Panshi Wang¹; Paul M. Montesano^{3,4}; Leonardo Calle⁵; Nuno Carvalhais^{6,7}; Benjamin Poulter^{8,9}; Matthew J. Macander¹⁰; Michael A. Wulder¹¹; Margaret Wooten^{3,12}; William Wagner^{3,12}; Akiko Elders¹³; Saurabh Channan¹; Christopher S.R. Neigh^{3,12}

Affiliations

¹ terraPulse, Inc., North Potomac, Maryland, USA.

² Institute of Tibetan Plateau Research, Chinese Academy of Sciences; Beijing, China.

³ NASA Goddard Spaceflight Center; Greenbelt, Maryland, USA.

⁴ ADNET Systems, Inc.; Bethesda, Maryland, USA.

⁵ calleEcology, Inc., Missoula, MT, USA.

⁶ Max Planck Institute for Biogeochemistry, Jena, Germany.

⁷ Departamento de Ciências e Engenharia do Ambiente, DCEA, Faculdade de Ciências e Tecnologia, FCT, Universidade Nova de Lisboa, Caparica, Portugal.

⁸ Spark Climate Solutions, San Francisco, California, USA.

⁹ Department of Geographical Sciences, University of Maryland, College Park, Maryland, USA.

¹⁰ ABR, Inc.—Environmental Research & Services, Fairbanks, Alaska, USA.

¹¹ Canadian Forest Service (Pacific Forestry Centre), Natural Resources Canada, 506 West Burnside Road, Victoria, British Columbia, Canada.

¹² Science Systems Applications, Inc., Lanham, Maryland, USA.

¹³ Morgan State University, Baltimore, Maryland, USA.

Correspondence to: Min Feng (mfeng@terrapulse.com), Joseph O. Sexton (sexton@terrapulse.com)



Abstract. The boreal forest has experienced the fastest warming of any forested biome in recent decades. While vegetation–climate models predict a northward migration of boreal tree cover, the long-term studies required to test the hypothesis have been confined to regional analyses, general indices of vegetation productivity, and data calibrated to other ecoregions. Here we report a comprehensive test of the magnitude, direction, and significance of changes in the distribution of the boreal forest based on the longest and highest-resolution time-series of calibrated satellite maps of tree cover to date. From 1985 to 2020, boreal tree cover expanded by 0.844 million km², a 12% relative increase since 1985, and shifted northward by 0.29° mean and 0.43° median latitude. Gains were concentrated between 64°–68°N and exceeded losses at southern margins, despite stable disturbance rates across most latitudes. Forest age distributions reveal that young stands (≤ 36 years) now comprise 15.4% of forest area and hold 1.1–5.9 Pg of aboveground biomass carbon, with the potential to sequester an additional 2.3–3.8 Pg C if allowed to mature. These findings confirm the global advance of the boreal forest and implicate the future importance of the region’s greening to the global carbon budget.

1 Introduction

The boreal biome is Earth’s most expansive and ecologically intact forest. The region contains 38 ± 3.1 Pg C of above-ground biomass (Neigh et al., 2013) and is underlain by 1672 Pg C, summing to total biomass rivaling the tropics and half of global soil C (Gauthier et al., 2015). Its forested area comprises a third of the global total and accounts for 20.8% of the total forest carbon (C) sink (Pan et al., 2011). Boreal tree cover also controls the reflective and thermal balance of solar radiation of the high northern latitudes, posing a positive feedback mechanism for greenhouse atmospheric warming (Betts, 2000; Bonan, 2008; Chen et al., 2018; Randerson et al., 2006).

The boreal region has experienced the fastest climatological warming of any forest biome, with annual surface temperatures increasing $> 1.4^\circ$ C over the past century (IPCC, 2014). Boreal forest dynamics are highly correlated to climate (Elmendorf et al., 2012; Holtmeier and Broll, 2005; Véga and St-Onge, 2009), and increases in vegetation productivity have been observed across the northern high latitudes (Berner and Goetz, 2022). However, regional increases in the frequency and severity of windthrow, fire, insect, and disease events have also been reported (Gauthier et al., 2015; Walker et al., 2019), and a recent analysis by Rotbarth et al. (2023) suggests that southern contraction exceeds northern expansion, yielding net shrinkage of the boreal forest.

While theory predicts a northward shift of the boreal forest, the global net effects of climate and other factors on the density and distribution of its tree cover remain untested hypotheses at the spatial and temporal scale of Landsat, Earth’s longest-running record of global, high-resolution satellite imagery. Coupled climate-vegetation models predict a net-northward migration of boreal vegetation due to warming (IPCC, 2018; Scheffer et al., 2012), supporting the dominance of growth processes. Multiple studies (Berner and Goetz, 2022; Sulla-Menashe et al., 2018; Zhu et al., 2016; Piao et al., 2020) have reported vegetation “greening” (e.g., Berner and Goetz, 2022) based on spectral indices of plant productivity. However, the ecological effects of trees differ from those of graminoids, shrubs, and other vegetation, and the comparatively low productivity of boreal ecosystems necessitate long-term analyses that have historically been limited to either regional scales or uncalibrated data (Beck et al., 2011; Brice et al., 2020; Taylor et



64 al., 2017; Rotbarth et al., 2023). As a result, the net effect of growth and mortality on the global distribution of boreal
65 tree cover, and the resulting effect on carbon budgets, remain uncertain.

66 Here we report a global test of the magnitude and direction of boreal-forest change from 1985 to 2020, as
67 observed through historical satellite records of tree cover calibrated to the boreal biome. We calibrated and expanded
68 a global tree cover dataset (Carroll et al. 2011, Sexton et al., 2013) to 224,026 Landsat images estimating tree cover
69 and its changes over the global extent of the boreal forest and adjacent tundra at annual, 30-meter resolution over 36
70 years (Fig. S1)—the most extensive and highest-resolution record of boreal tree cover to date. This pan-boreal time
71 series was then subjected to trend analysis to estimate and map the historical direction, rate, and significance of change
72 across the region, and the resulting estimates of forest age were used to infer impacts on the region’s carbon budget.

73

74 **2 Methods**

75 **2.1 Historical retrieval of tree cover**

76 To improve characterization of boreal forest structure, we calibrated the 250-m resolution, 2000 - 2020 MODIS
77 Vegetation Continuous Fields (VCF) Tree Cover product (MOD44B Collection 6; Carroll et al., 2011) against a
78 region-wide sample of airborne lidar measurements, stratifying by topographic and bioclimatic covariates (SI §2–4).
79 This boreal-specific calibration improved characterization of tree-cover gradients across the boreal region (Fig. S7),
80 increasing accuracy, decreasing uncertainty, and improving the linear correlation of per-pixel fractional tree cover
81 estimates to reference measurements (Fig. S8). Mean absolute error (MAE) decreased to 11.13%, root-mean-squared
82 error (RMSE) decreased to 16.44%, and the coefficient of determination (R^2) of the linear model between estimated
83 and measured data increased to 0.60. Following calibration, the calibrated MODIS VCF estimates were downscaled
84 to 30-meter resolution and extended from 1984 to 2020 following Sexton et al. (2013). The residual bias of the
85 Landsat-based estimates relative to the lidar reference measurements was slight (~2%, SI).

86 Calibrated MODIS VCF estimates were then downscaled to 30-m resolution and extended to 1984–2020 by
87 applying a machine learning model (gradient-boosted regression tree) to Landsat surface reflectance imagery from
88 sensors TM, ETM+, and OLI (Sexton et al., 2013; SI §5–6). A total of 224,026 Landsat scenes across 2,189 WRS-2
89 tiles was used to reconstruct annual tree cover estimates, composited to minimize cloud, snow, and phenological noise.
90 For each pixel-year, the median value of valid observations was retained, resulting in a consistent, high-resolution
91 time series of tree cover estimates (Fig. S5–S7).

92

93 **2.2. Tree cover trend analysis**

94 Calibrated, downscaled, and extended tree cover values were then summarized across the region as annual, boreal-
95 wide means and medians to calculate changes over the 36-year study span (Fig. 2). The annual mean and median tree
96 cover were also broken down by latitude to calculate the change rate at each latitudinal degree between 47°N to 70°N
97 (Fig. S10). Cover estimates for 1984 were excluded from the trend analysis due to the poor spatial coverage in the
98 first operational year of Landsat 5 (Fig. S2), and pixels with ≤ 30 unobscured annual tree cover observations were
99 excluded to minimize unbalanced representation caused by the lapses in the availability of Landsat images, mainly in
100 central and northeast Siberia (Neigh et al., 2013; Sexton et al., 2013).



101

102 **2.3. Detection of forest change and estimation of age**

103 Following the United Nations Framework Convention on Climate Change (UNFCCC, 2002), forest was defined as
104 tree cover exceeding 30% within each 30-m pixel. The probability of a pixel being forested, $p(F)$, was calculated as
105 the integral of the probability density function of tree cover values exceeding this 30% threshold (SI §11). Using the
106 36-year time series of annual, 30-m resolution estimates of forest probability ($p(F)$), gains and losses were identified
107 by applying a two-sample z-test in a moving kernel centered on transitions across the 50% threshold of $p(F)$ (Fig.
108 S13).

109 Pixels with multiple statistically significant transitions during the 1985–2020 period were permitted up to
110 three gain or loss events. Disturbances were classified as “complete” if ≤ 7 years of data were missing, and “incomplete”
111 otherwise. Incomplete disturbances were concentrated in areas with sparse Landsat acquisitions prior to 1999, before
112 implementation of systematic global imaging by Landsat 7 (Sexton et al., 2013; Potapov et al., 2012).

113 Forest age was estimated for each year and pixel by subtracting the year of the most recent significant forest gain from
114 the year of interest. Pixels were classified as “new” forests if no forest cover or loss had been observed earlier in the
115 time series within a 150-m radius (five Landsat pixels); otherwise, forests were considered “recovering.” Accuracy of
116 change detection and age estimation was assessed against a reference sample of 2,404 visually interpreted points
117 distributed across the boreal biome (SI Fig. S14–S15).

118

119 **2.4. Estimation of aboveground biomass**

120 Aboveground biomass carbon (AGB) was estimated as a function of forest stand age using a linear growth model
121 (Cook-Patton et al., 2020; Fig. S16), with intercept ($\mu = -35.7$, $\sigma = 12.6$) and slope coefficients ($\mu = 23.2$, $\sigma = 3.2$)
122 incorporating parametric uncertainty. Because ages of forests older than the 36-year time-series could not be directly
123 observed, we assumed three scenarios of stand age to bracket carbon stock estimates in these undated stands: 36 years
124 yielding 19.1–58.4 Pg C, 100 years yielding 35.8–80.5 Pg C, and 300 years yielding 42.4–89.2 Pg C. These scenarios
125 define the plausible envelope of legacy biomass in mature forest. However, estimates reflected structural biomass only
126 and did not account for potential effects of changes in soil moisture or variation in respiration rates. To contextualize
127 the biomass sink relative to climate-driven emissions, we also evaluated the trend in regional surface air temperature
128 using two reanalysis products. Both records indicated significant warming over the study period, with trends of
129 $0.038^{\circ}\text{C yr}^{-1}$ ($r = 0.69$, $p < 1 \times 10^{-5}$) and $0.035^{\circ}\text{C yr}^{-1}$ ($r = 0.73$, $p < 1 \times 10^{-6}$) respectively (Fig. S17).

130 **3 Results**

131 **3.1. Distribution of boreal tree cover**

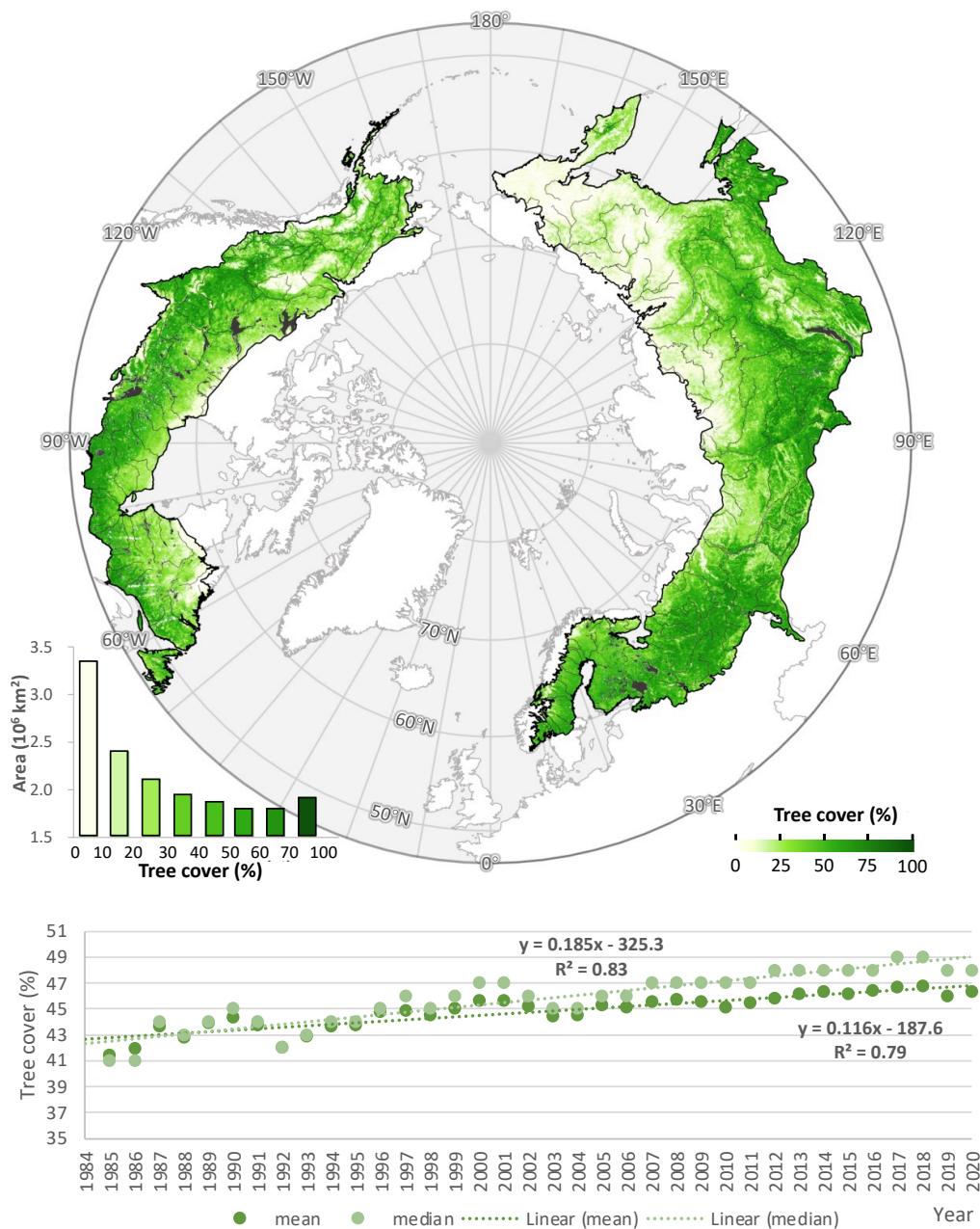
132 Tree cover reaches its highest densities in the southern portion of the boreal biome and decreases progressively
133 northward (Fig. 1). Sparse conifer stands, woodlands, herbaceous vegetation, and unvegetated barrens dominate the
134 transition to Arctic tundra, and tree cover is nearly absent north of 71°N . Due to interspersed of tundra, wetlands, and
135 inland water bodies, the most common local (i.e., 30-meter pixel) tree-cover density across the entire boreal forest and
136 taiga-tundra ecotone is below 5%



137 From 1985 to 2020, boreal tree cover increased by 0.844 million km², a 4.3 percentage point absolute increase
138 and a 12% relative increase over its 1985 extent (Fig. 1). Tree cover expanded from 7.153 million km² (41.44% of the
139 region) in 1985 to 7.997 million km² (46.32%) in 2020, with a linear trend of 0.023 million km² yr⁻¹ (0.12% yr⁻¹;
140 percent cover = $0.116 \times \text{year} - 187.6$, $R^2 = 0.99$, $p < 0.001$). Applying the UNFCCC forest definition of 10–30% tree
141 cover (UNFCCC, 2002; Sexton et al., 2016), the region held between 8.95 and 12.41 million km² of forest in 2000
142 and between 9.41 and 13.26 million km² in 2020.

143 The latitudinal distribution of tree cover also shifted northward from 1985 to 2020. The mean latitude of tree
144 cover increased by 0.29°, from 57.37°N in 1985 to 57.66°N in 2020 (mean latitude = $0.0075 \times \text{year} + 42.6$, $R^2 = 0.79$,
145 $p < 0.001$). The median latitude increased more rapidly, by 0.43° (median latitude = $0.0124 \times \text{year} + 32.5$, $R^2 = 0.88$,
146 $p < 0.001$), indicating widespread net expansion across the biome rather than outliers of change at either its northern
147 or southern extremes.

148



149

150

151

152

153

154

Fig. 1. Distribution of tree cover across boreal and arctic tundra ecoregions in 2020. Estimates from 2020 are shown. Data gaps due to clouds were filled with estimates from earlier years. Ecoregions were defined by Dinerstein et al (2017). The bottom panel shows the increasing density in the overall, pan-boreal density of tree cover from 1985 to 2020.



3.2. The pace and pattern of boreal forest change

Net biome-wide changes were underlain by strong geographic variation (Fig. 2). Net gains from 1985 to 2020 occurred at all latitudes above 53°N, with the strongest increases concentrated between 64° and 68°N. Gains in the northernmost latitudes support the hypothesis of a poleward shift in the northernmost extent of tree cover and are consistent with findings by Montesano et al. (2024), who reported long-term increases in deciduous and mixed forest components in transitional boreal zones. These structural shifts parallel recent evidence that warming-induced species diversification is strongest near the tundra margin as temperate species colonize newly viable habitat (Xi et al., 2024). In contrast, net losses were smaller in magnitude and limited to the southern boreal latitudes (47°–52°N), corroborating recent observations by Rotbarth et al. (2023) (Fig. 3).

Our analysis of calibrated, high (30-meter) resolution estimates of tree cover minimized potential for herbaceous growth to obscure tree mortality, for which coarser-resolution, NDVI-based analyses have been criticized (Yan et al., 2024). The pan-boreal expansion of tree cover occurred against relatively stable disturbance rates over the study period (Fig. 3), and observed disturbances influenced regional patterns but did not obscure the biome-wide trend. The annual rate of disturbance increased modestly from 53,546 km² yr⁻¹ in 2000 to 60,275 km² yr⁻¹ in 2020, equivalent to a 1.8% yr⁻¹ increase (1,100 km² yr⁻¹), or approximately 0.2%–0.4% of the forested area. Locations undisturbed between 1985 and 2020 exhibited net gains across nearly all latitudes, and the latitudinal distribution of disturbance—while varying strongly among years—remained broadly stationary over time. (Fig. S10).

In North America, the largest gains were concentrated in the northernmost boreal, where increases in shrubs and grasses have also been reported (McManus et al., 2012). Areas of net loss corresponded to widespread forest disturbances, including wildfire and bark beetle (*Dendroctonus* spp.) outbreaks in British Columbia (Meddens et al., 2012), spruce budworm (*Choristoneura* spp.) in Quebec (Boulanger and Arseneault, 2004), and wildfire across western Canada and interior Alaska (Stocks et al., 2002). Recent shifts in transitional forest structure and composition noted by Montesano et al. (2024) lend further weight to these observations, suggesting a biome-wide response in functional traits, including increased deciduous dominance at the taiga-tundra ecotone. These findings are also partially corroborated by Rotbarth et al. (2023), who also reported tree cover gains in the boreal interior of North America but loss at the southern margins, especially in areas impacted by wildfire and harvest.

In Eurasia, hotspots of forest loss included the eastern Russian–Chinese border, agricultural zones south of the Urals, and regions affected by timber harvesting near the Russia–Finland border in the 1990s (Potapov et al., 2012). Logging and fire contributed to localized loss in eastern Russia (Krylov et al., 2014), whereas gains in northern Europe were associated with silvicultural management, afforestation, and fire suppression (Henttonen et al., 2017). Recent analyses confirm extensive regrowth in post-agricultural and permafrost-transitioning landscapes in Russia, where lidar and optical remote sensing reveal increases in regeneration potential, particularly in abandoned or disturbed sites (Neigh et al., 2025).

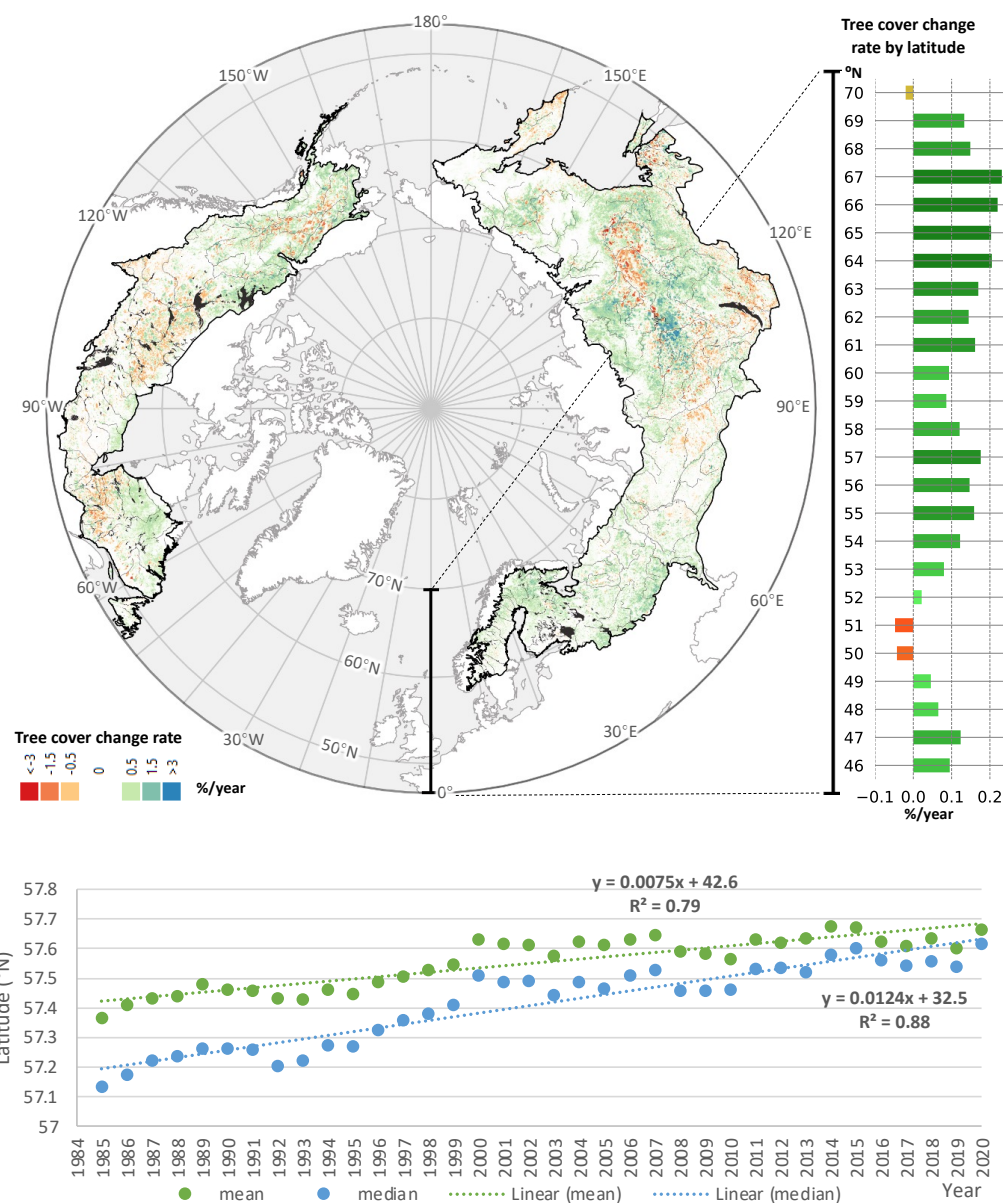
In Asia, net gains were observed in areas of post-Soviet agricultural abandonment, as well as in larch forests near the Yakutsk permafrost zone. These trends are consistent with increases in tall shrubs and larch (*Larix* spp.) at the taiga–tundra boundary (Frost and Epstein, 2014). Recovery from wildfires in the 1990s continues in these regions (Kajii et al., 2002), and permafrost thaw has been hypothesized to enhance productivity (Sato et al., 2016).



192 Although we did not attempt to demarcate or detect changes in a discrete tree line, our observations
193 corroborate the boreal advancement hypothesis alongside field measurements of woody vegetation near the northern
194 limits of tree growth and satellite-based studies demarcating the northern tree line (Frost and Epstein, 2014; Rees et
195 al., 2020; Dial et al., 2024; Dial et al., 2022; Rotbarth et al. 2023). While analysis of tree-cover estimates avoided the
196 potential confusion of changes in trees specifically with general NDVI-based “greening” (Yan et al. 2024), the trend’s
197 geographic variations correspond to general patterns of greening across the biome (Berner and Goetz, 2022; Sulla-
198 Menashe et al., 2018; Zhu et al., 2016; Piao et al., 2020; Guay et al., 2014).

199 Field studies have shown that climate, soil properties, and forest management drive large differences in boreal
200 tree growth rates across the ecotone (Henttonen et al., 2017; Henttonen et al., 2017; Hofgaard et al., 2009). Recent
201 shifts in transitional forest structure and composition noted by Montesano et al. (2024) lend further weight to these
202 observations, suggesting a total biome-wide response in functional traits, including increased deciduous dominance
203 near treeline margins. Xi et al. (2024) further demonstrate that increasing diversity near the forest–tundra boundary is
204 associated with moderate climatic warming, although they caution that the gains are vulnerable to reversal under
205 extremes such as drought and heatwaves. Changes in species composition remain a focal point of research (Xi et al.,
206 2024; Mekonnen et al., 2019; Massey et al., 2023; Mack et al., 2021; Liski et al., 2003), while still remaining to be
207 explored are the differentiation of climate and soil effects at the global scale and the discrimination of tree cover
208 expansion due to the establishment and growth of new seedlings versus the widening of existing tree crowns.

209



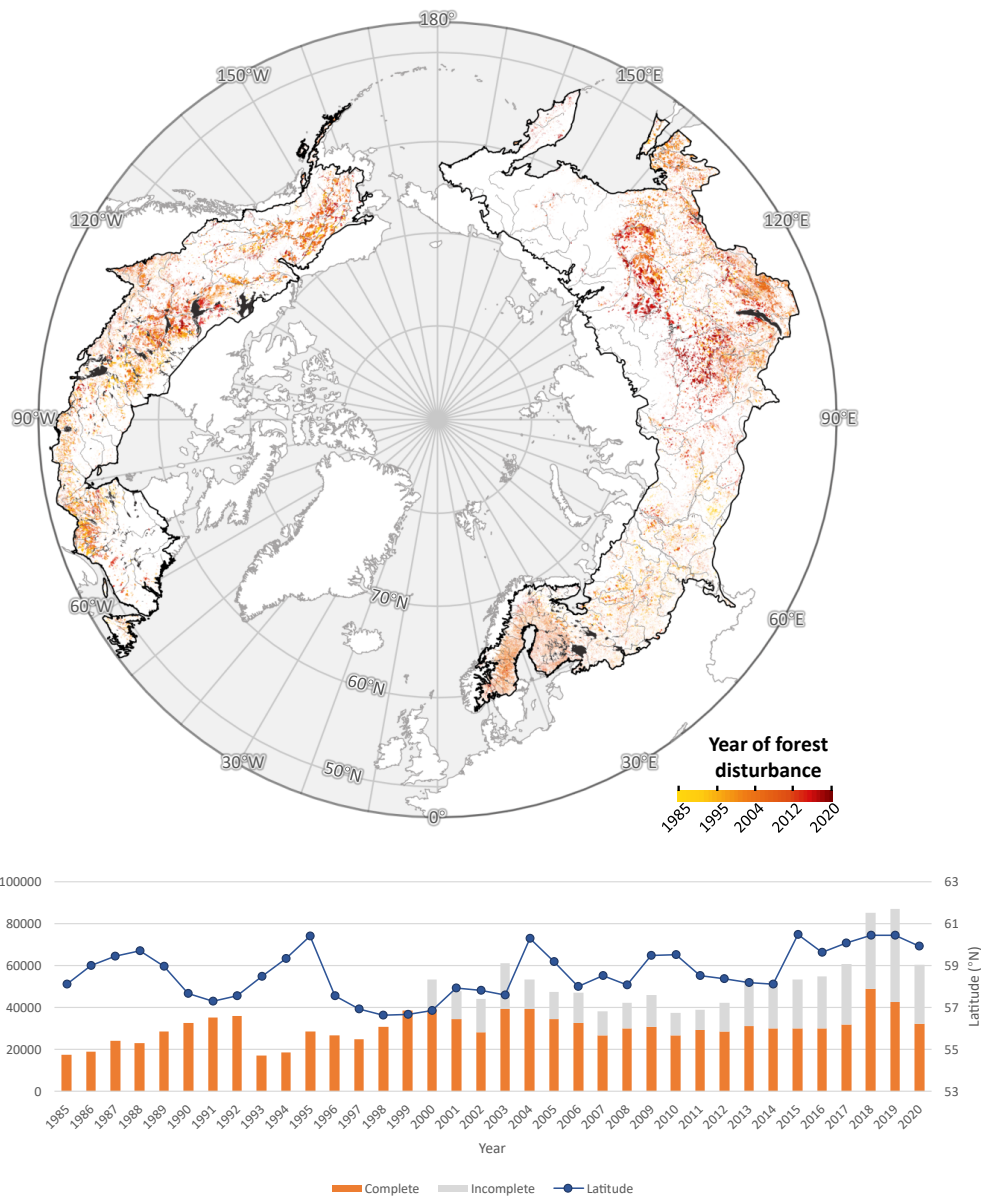


Fig. 3. Total area and median latitude of boreal stand-clearing disturbances from 1985 to 2020. Trends are plotted for the portion of the boreal area where the satellite image is complete from 1984 to 2019 (“complete”) and from all locations, including where the satellite record is incomplete (“incomplete”) (Supplemental Information).



224 **3.3. The distribution of boreal forest age**

225 Most of the boreal forest—8.19 million km², or 47.5% of the region—is older than can be directly measured from the
226 satellite record (Fig. 4). Tree cover in these older stands was already established by the beginning of the Landsat
227 observation period in 1985, and the slow rates of biomass accumulation in boreal ecosystems further complicate the
228 detection of recent forest establishment (SI Fig. S15). However, the age of younger stands can be estimated by
229 subtracting the year of first detected forest cover from 2020.

230 Of the forested area present in 1985, 0.5 million km²—representing 5.29% of standing forests—was disturbed
231 during the study period and recovered to forest by 2020. Recovering forests, combined with “new” forests gained
232 during the Landsat era, produced a weak modal age class centered between 9 and 21 years, with a notable lapse in the
233 youngest age classes. These young forests were concentrated in regions of intensive silviculture, including industrial
234 plantations in Scandinavia (Henttonen et al., 2017; Liski et al., 2003; Ågren et al., 2008), and in areas recovering from
235 wildfire. The latter trend is corroborated by reports of increasing burn frequency and extent in Siberia since the late
236 20th century (Kharuk et al., 2021), which has driven a rising proportion of recovering forest younger than 20 years.

237

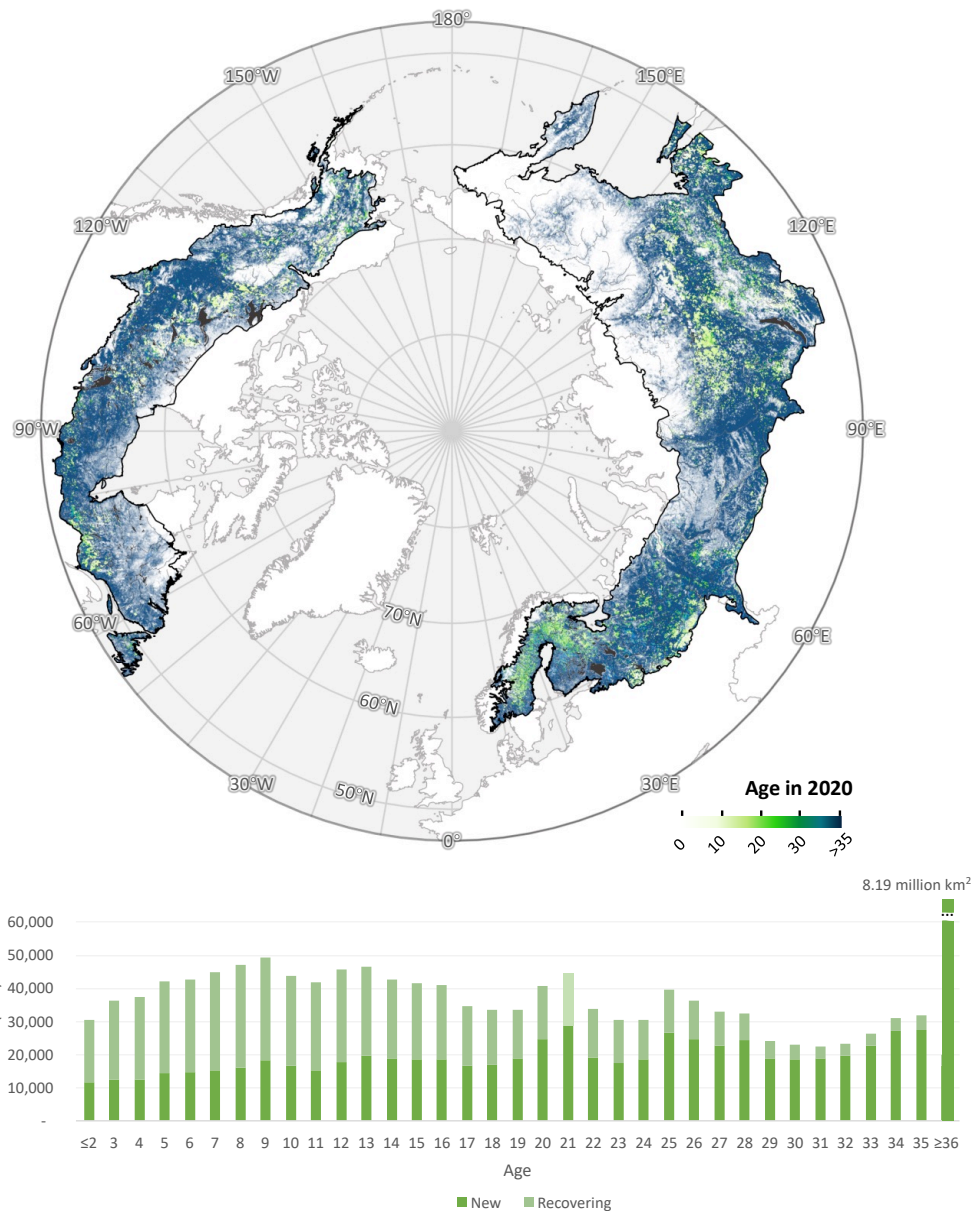


Fig. 4. Spatial distribution of stand age (top) across the boreal ecoregion and frequency distribution of boreal stand age in 2020 (bottom). Forest age-class distribution is defined as years since establishment of pixels identified as forest in 2020. “New” forests were identified as pixels with forest cover following a gain but no prior forest cover or loss earlier in the time series within a 150-m radius (5 pixels) over the observable period (1984 – 2020); “recovering” forests were identified as pixels with forest cover following a gain where a forest loss had been observed previously in the series (Supplemental Information).



247 4 Discussion

248 The expansion and redistribution of boreal tree cover documented in this study has direct implications for the region's
249 role in the global carbon cycle. Between 1985 and 2020, boreal tree cover increased by 0.844 million km² and shifted
250 northward by over 0.4° in median latitude, with gains concentrated at the biome's northern margin and net expansion
251 observed across most latitudes. These changes are not only spatially extensive but demographically consequential:
252 they reflect a growing fraction of young forests with distinct structural and functional attributes that position them as
253 dynamic agents of carbon sequestration. Understanding the contribution of these forests to current and future carbon
254 stocks is essential for anticipating the net climate feedbacks emerging from boreal ecosystems.

255 Recent models relating forest age to biomass dynamics suggest that shifting age structure will substantially
256 influence the boreal region's contribution to the global carbon budget in the coming decades. Young forests already
257 contribute significantly to the region's carbon sink (Pan et al., 2011). Forests with known stand ages (≤ 36 years since
258 disturbance) hold between 1.1 and 5.9 Pg C in aboveground biomass, based on global growth models (Cook-Patton et
259 al., 2020). The ages of forests where no disturbance was observed during the satellite era remain unknown, but
260 plausible aboveground carbon stocks in these older stands can be bracketed between a low-end scenario assuming 36
261 years of age (19.1–58.4 Pg C) and a high-end scenario assuming 300 years (42.4–89.2 Pg C). Based on these estimates,
262 forests ≤ 36 years of age comprise 1.35–14.20% of the total boreal aboveground biomass carbon stock—consistent
263 with their 15.4% share of total forest area. Including belowground biomass would raise these values by approximately
264 25%, based on a mean global root:shoot ratio of 0.25 (Huang et al., 2021).

265 If allowed to mature without further disturbance, these young forests could sequester an additional 2.3–3.8
266 Pg C in aboveground biomass. Forests newly established during the observation period contribute between 0.8 and
267 3.5 Pg C today, exceeding the 0.3–2.4 Pg C held in forests recovering from recorded disturbances. Over the next 36
268 years, new forests represent a potential additional aboveground sink of 1.3–2.0 Pg C (0.036–0.18 Pg C yr⁻¹), compared
269 to 1.0–1.8 Pg C (0.028–0.05 Pg C yr⁻¹) from recovering forests. This distinction reflects both the greater area occupied
270 by new forests (7.6% vs. 6.7%) and their older mean stand age. These findings support recent observations by Neigh
271 et al. (2025), who reported a disproportionately large contribution of young, regrowing stands to carbon storage in the
272 Russian boreal.

273 The additional carbon in new forests could help offset warming-induced increases in boreal ecosystem
274 respiration, which have been estimated between 5 and 28 Pg C from 1985 to 2020 (SI Fig. S16). Both climate warming
275 and CO₂ fertilization are expected to enhance productivity (Norby and Zak, 2011), and the spatial pattern of observed
276 tree-cover growth aligns with model predictions of increased seasonal CO₂ exchange above 40°N (Forkel et al., 2016).
277 However, several mechanisms may limit this offset. First, temperature sensitivity of respiration can itself be
278 temperature-dependent (Koven et al., 2017). Second, carbon accumulation rates decline with forest age (Odum, 1969).
279 Third, thawing of permafrost can release substantial legacy carbon stocks (Schuur et al., 2015). Fourth, increases in
280 fire and harvest activity may reverse regional gains in biomass (Gauthier et al., 2015; Kharuk et al., 2021).
281 Compositional and functional transitions may also alter sink dynamics (Montesano et al., 2024; Xi et al., 2024).

282 The long-term persistence of tree-cover expansion depends not only on productivity, but also on the capacity
283 of boreal soils to support woody vegetation. It remains uncertain whether boreal soils—especially under changing



284 permafrost regimes—can structurally sustain expanded forest cover (Koven, 2013). Additional uncertainty stems from
285 the rising role of anthropogenic fire in some parts of the boreal zone (Doerr and Santin, 2016; Mollicone et al., 2006).
286 Our biomass estimates are derived from models for natural forests and do not account for differences between managed
287 and unmanaged systems (Kuuluvainen and Gauthier, 2018) or for anticipated changes in fire regimes.

288 While expansion of tree cover may imply increased carbon storage, nonlinear biodiversity responses to
289 warming complicate projections. Enhanced taxonomic and functional diversity may improve ecological resilience (Xi
290 et al., 2024), but these benefits are constrained by the growing frequency of climatic extremes. Moreover, biodiversity-
291 related feedbacks on carbon balance remain difficult to predict under scenarios of increasing disturbance. Ultimately,
292 all of these processes—forest growth, mortality, disturbance, and compositional change—are already underway across
293 the boreal biome. Quantifying the balance of autotrophic and heterotrophic carbon fluxes remains critical to
294 understanding and managing the global climate system.

295 **Conclusions**

296 This pan-boreal assessment provides the strongest empirical confirmation to date of a northward shift in boreal tree
297 cover, long hypothesized by climate–vegetation models. By retrieving the longest, highest-resolution, and most
298 spatially complete record of calibrated boreal tree cover available, we applied machine learning to the Landsat archive
299 to reconstruct annual, 30-m maps of forest change from 1985 to 2020. Time-series analysis of 1.9×10^8 pixels revealed
300 widespread increases in tree-cover density and a poleward shift in forest distribution, occurring despite relatively
301 stable disturbance rates across the biome.

302 Although the net trends are globally significant, they mask substantial geographic and temporal heterogeneity,
303 as well as complexity in the ecological processes underlying forest change. These results underscore the need for high-
304 resolution, disturbance-aware metrics to supplement NDVI-based assessments, particularly in climatically sensitive
305 boreal transition zones (Yan et al., 2024). A more complete understanding of boreal forest dynamics will require
306 integration of satellite time series with field-based measurements of canopy structure and the environmental drivers
307 of growth, mortality, and species turnover. Moreover, translating the resulting information into action to forestall and
308 adapt to climate change will require effective communication across scientific, government, and commercial domains
309 of human activity.

310 **Acknowledgments**

311 This research was supported by the NASA Carbon Cycle Science Program (NNH16ZDA001N-CARBON), National
312 Science Foundation Arctic System Science Program (1604105), and NASA ABoVE (80NSSC19M0112). Satellite
313 image processing was performed by terraPulse, Inc. on Amazon Web Services (AWS). Reference data for calibration
314 and validation was produced on the NASA Goddard Spaceflight Center ADAPT and HEC clusters. Aaron Wells (ABR,
315 Inc.), Celio De Sousa (NASA Goddard Space Flight Center, URSA, Inc.), and Jaime Nickeson (NASA Goddard Space
316 Flight Center, SSAI, Inc.) contributed reference observations of forest cover and disturbance. Resources supporting



317 this work were provided by the NASA High-End Computing Program through the NASA Center for Climate
318 Simulation at Goddard Space Flight Center.

319 **Author Contributions**

320 MF and JS designed and developed the tree-cover and forest-change algorithms. PM, PW, and MM conducted the
321 validation and calibration. CN and PM co-edited the manuscript, CN secured research funding to conduct the
322 study. BP commented on the final manuscript. NC and LC conducted the carbon impact analysis. NC conducted the
323 ecosystem respiration analysis. SC developed the platform on AWS. MW, WW, and AE interpreted the validation
324 dataset. JS conceived the study and compiled the manuscript with contributions from all coauthors.

325

326 **References**

- 327 Ågren, G. I., Hyvönen, R., and Nilsson, T.: Are Swedish forest soils sinks or sources for CO₂—model analyses based
328 on forest inventory data, *Biogeochemistry*, 89, 139–149, <https://doi.org/10.1007/s10533-007-9121-0>, 2008.
- 329 Baltzer, J. L., Alexander, H. D., Greaves, H. E., Boulanger, Y., Gauthier, S., Fuller, M. M., and Beck, P. S. A.:
330 Increasing fire and the decline of fire-adapted black spruce in the boreal forest, *Proc. Natl. Acad. Sci. USA*, 118,
331 e2024872118, <https://doi.org/10.1073/pnas.2024872118>, 2021.
- 332 Beck, P. S. A., Juday, G. P., Alix, C., Barber, V. A., Winslow, S. E., Sousa, E. E., Heiser, P., Herriges, J. D., and
333 Goetz, S. J.: Changes in forest productivity across Alaska consistent with biome shift, *Ecol. Lett.*, 14, 373–379,
334 <https://doi.org/10.1111/j.1461-0248.2011.01598.x>, 2011.
- 335 Berner, L. T., and Goetz, S. J.: Satellite observations document trends consistent with a boreal forest biome shift, *Glob.*
336 *Change Biol.*, 28, 3275–3292, <https://doi.org/10.1111/gcb.16100>, 2022.
- 337 Betts, R. A.: Offset of the potential carbon sink from boreal forestation by decreases in surface albedo, *Nature*, 408,
338 187–190, <https://doi.org/10.1038/35041545>, 2000.
- 339 Bonan, G. B.: Forests and climate change: Forcings, feedbacks, and the climate benefits of forests, *Science*, 320,
340 1444–1449, <https://doi.org/10.1126/science.1155121>, 2008.
- 341 Boulanger, Y., and Arseneault, D.: Spruce budworm outbreaks in eastern Quebec over the last 450 years, *Can. J. For.*
342 *Res.*, 34, 1035–1043, <https://doi.org/10.1139/x03-269>, 2004.
- 343 Brice, M., Boucher, Y., Girardin, M. P., Marchand, W., Tremblay, J.-P., and Krause, C.: Moderate disturbances
344 accelerate forest transition dynamics under climate change in the temperate–boreal ecotone of eastern North America,
345 *Glob. Change Biol.*, 26, 4418–4435, <https://doi.org/10.1111/gcb.15115>, 2020.



- 346 Bunn, A. G., and Goetz, S. J.: Trends in satellite-observed circumpolar photosynthetic activity from 1982 to 2003:
347 The influence of seasonality, cover type, and vegetation density, *Earth Interact.*, 10, 1–19,
348 <https://doi.org/10.1175/EI190.1>, 2006.
- 349 Carroll, M., DiMiceli, C., Sohlberg, R., Huang, C., and Hansen, M. C.: MODIS Vegetative Cover Conversion and
350 Vegetation Continuous Fields, in: *Land Remote Sensing and Global Environmental Change: NASA’s Earth Observing*
351 *System and the Science of ASTER and MODIS*, edited by: Ramachandran, B., Justice, C. O., and Abrams, M. J., 725–
352 745, Springer, New York, NY, https://doi.org/10.1007/978-1-4419-6749-7_32, 2011.
- 353 Chen, D., Loboda, T. V., He, T., Zhang, Y., and Liang, S.: Strong cooling induced by stand-replacing fires through
354 albedo in Siberian larch forests, *Sci. Rep.*, 8, 4821, <https://doi.org/10.1038/s41598-018-23050-9>, 2018.
- 355 Ciais, P., Yao, Y., Gasser, T., Baccini, A., Wang, Y., Lauerwald, R., Peng, S., Bastos, A., Cescatti, A., and Yue, C.:
356 Five decades of northern land carbon uptake revealed by the interhemispheric CO₂ gradient, *Nature*, 568, 221–225,
357 <https://doi.org/10.1038/s41586-019-1078-6>, 2019.
- 358 Cook-Patton, S. C., Leavitt, S. M., Gibbs, D., Harris, N. L., Lister, K., Anderson-Teixeira, K. J., Briggs, R. D.,
359 Chazdon, R. L., Crowther, T. W., and Ellis, P. W.: Mapping carbon accumulation potential from global natural forest
360 regrowth, *Nature*, 585, 545–550, <https://doi.org/10.1038/s41586-020-2686-x>, 2020.
- 361 Dial, R. J., Beamer, J. P., McDowell, P. D., Herriott, I. C., Milne, B. T., Giardina, C. P., and Sullivan, P. F.: Arctic
362 sea ice retreat fuels boreal forest advance, *Science*, 383, 877–884, <https://doi.org/10.1126/science.adj0832>, 2024.
- 363 Dial, R. J., Maher, C. T., Hewitt, R. E., and Sullivan, P. F.: Sufficient conditions for rapid range expansion of a boreal
364 conifer, *Nature*, 608, 546–551, <https://doi.org/10.1038/s41586-022-05066-4>, 2022.
- 365 Dinerstein, E., Olson, D., Joshi, A., Vynne, C., Burgess, N. D., Wikramanayake, E., Hahn, N., Palminteri, S., Hedao,
366 P., and Noss, R.: An ecoregion-based approach to protecting half the terrestrial realm, *BioScience*, 67, 534–545,
367 <https://doi.org/10.1093/biosci/bix014>, 2017.
- 368 Doerr, S. H., and Santín, C.: Global trends in wildfire and its impacts: perceptions versus realities in a changing world,
369 *Philos. Trans. R. Soc. B Biol. Sci.*, 371, 20150345, <https://doi.org/10.1098/rstb.2015.0345>, 2016.
- 370 Elmendorf, S. C., Henry, G. H. R., Hollister, R. D., Björk, R. G., Bjorkman, A. D., Callaghan, T. V., and Collier, L.
371 S.: Plot-scale evidence of tundra vegetation change and links to recent summer warming, *Nat. Clim. Change*, 2, 453–
372 457, <https://doi.org/10.1038/nclimate1465>, 2012.
- 373 Forkel, M., Carvalhais, N., Rödenbeck, C., Keeling, R., Heimann, M., Thonicke, K., Reichstein, M., and High-
374 Latitude Ecosystem Modeling Group: Enhanced seasonal CO₂ exchange caused by amplified plant productivity in
375 northern ecosystems, *Science*, 351, 696–699, <https://doi.org/10.1126/science.aac4971>, 2016.
- 376 Frost, G. V., and Epstein, H. E.: Tall shrub and tree expansion in Siberian tundra ecotones since the 1960s, *Glob.*
377 *Change Biol.*, 20, 1264–1277, <https://doi.org/10.1111/gcb.12406>, 2014.



- 378 Gauthier, S., Bernier, P., Kuuluvainen, T., Shvidenko, A. Z., and Schepaschenko, D. G.: Boreal forest health and
379 global change, *Science*, 349, 819–822, <https://doi.org/10.1126/science.aaa9092>, 2015.
- 380 Guay, K. C., Beck, P. S. A., Berner, L. T., Goetz, S. J., Baccini, A., and Buermann, W.: Vegetation productivity
381 patterns at high northern latitudes: a multi-sensor satellite data assessment, *Glob. Change Biol.*, 20, 3147–3158,
382 <https://doi.org/10.1111/gcb.12647>, 2014.
- 383 Henttonen, H. M., Nöjd, P., and Mäkinen, H.: Environment-induced growth changes in the Finnish forests during
384 1971–2010 – An analysis based on National Forest Inventory, *For. Ecol. Manag.*, 386, 22–36,
385 <https://doi.org/10.1016/j.foreco.2016.12.021>, 2017.
- 386 Hofgaard, A., Dalen, L., and Hytteborn, H.: Tree recruitment above the treeline and potential for climate-driven
387 treeline change, *J. Veg. Sci.*, 20, 1133–1144, <https://doi.org/10.1111/j.1654-1103.2009.01106.x>, 2009.
- 388 Holtmeier, F.-K., and Broll, G.: Sensitivity and response of northern hemisphere altitudinal and polar treelines to
389 environmental change at landscape and local scales, *Glob. Ecol. Biogeogr.*, 14, 395–410,
390 <https://doi.org/10.1111/j.1466-822X.2005.00168.x>, 2005.
- 391 Huang, Y., Crowther, T. W., and Maynard, D. S.: A global map of root biomass across the world’s forests, *Earth Syst.*
392 *Sci. Data*, 13, 4263–4274, <https://doi.org/10.5194/essd-13-4263-2021>, 2021.
- 393 IPCC: Climate Change 2014 Synthesis Report, IPCC, Geneva, Switzerland, 2014.
- 394 IPCC: Global Warming of 1.5°C, IPCC Special Report, 2018.
- 395 Ju, J., and Masek, J. G.: The vegetation greenness trend in Canada and US Alaska from 1984–2012 Landsat data,
396 *Remote Sens. Environ.*, 176, 1–16, <https://doi.org/10.1016/j.rse.2016.01.001>, 2016.
- 397 Kajii, Y., Kato, S., Streets, D. G., Tsai, N. Y., Shibata, T., Matsumoto, J., and Kajino, M.: Boreal forest fires in Siberia
398 in 1998: Estimation of area burned and emissions of pollutants by advanced very high resolution radiometer satellite
399 data, *J. Geophys. Res. Atmospheres*, 107, ACH 4-1–ACH 4-8, <https://doi.org/10.1029/2001JD001078>, 2002.
- 400 Kharuk, V. I., Ponomarev, E. I., Ivanova, G. A., Dvinskaya, M. L., Coogan, S. C. P., and Flannigan, M. D.: Wildfires
401 in the Siberian taiga, *Ambio*, <https://doi.org/10.1007/s13280-020-01490-x>, 2021.
- 402 Koven, C. D.: Boreal carbon loss due to poleward shift in low-carbon ecosystems, *Nat. Geosci.*, 6, 452–456,
403 <https://doi.org/10.1038/ngeo1801>, 2013.
- 404 Koven, C. D., Hugelius, G., Lawrence, D. M., and Wieder, W. R.: Higher climatological temperature sensitivity of
405 soil carbon in cold than warm climates, *Nat. Clim. Change*, 7, 817–822, <https://doi.org/10.1038/nclimate3421>, 2017.
- 406 Krylov, A., McCarty, J. L., Potapov, P., Loboda, T., Tyukavina, A., Turubanova, S., and Hansen, M. C.: Remote
407 sensing estimates of stand-replacement fires in Russia, 2002–2011, *Environ. Res. Lett.*, 9, 105007,
408 <https://doi.org/10.1088/1748-9326/9/10/105007>, 2014.
- 409 Kuuluvainen, T., and Gauthier, S.: Young and old forest in the boreal: critical stages of ecosystem dynamics and
410 management under global change, *For. Ecosyst.*, 5, 26, <https://doi.org/10.1186/s40663-018-0149-8>, 2018.



- 411 Liski, J., Perruchoud, D., Karjalainen, T., and Poulton, P.: Increased carbon sink in temperate and boreal forests, *Clim.*
412 *Change*, 61, 89–109, <https://doi.org/10.1023/A:1026368803516>, 2003.
- 413 Mack, M. C., Walker, X. J., Johnstone, J. F., Alexander, H. D., Melvin, A. M., Miller, S. N., and Goetz, S. J.: Carbon
414 loss from boreal forest wildfires offset by increased dominance of deciduous trees, *Science*, 372, 280–283,
415 <https://doi.org/10.1126/science.abf3903>, 2021.
- 416 Massey, R., Walker, X. J., Mack, M. C., Johnstone, J. F., Miller, S. N., and Goetz, S. J.: Forest composition change
417 and biophysical climate feedbacks across boreal North America, *Nat. Clim. Change*, 13, 1368–1375,
418 <https://doi.org/10.1038/s41558-023-01826-4>, 2023.
- 419 McManus, K. M., Morton, D. C., Masek, J. G., Wang, D., Sexton, J. O., and Nagol, J.: Satellite-based evidence for
420 shrub and graminoid tundra expansion in northern Quebec from 1986 to 2010, *Glob. Change Biol.*, 18, 2313–2323,
421 <https://doi.org/10.1111/j.1365-2486.2012.02708.x>, 2012.
- 422 Meddens, A. J. H., Hicke, J. A., and Ferguson, C. A.: Spatiotemporal patterns of observed bark beetle-caused tree
423 mortality in British Columbia and the western United States, *Ecol. Appl.*, 22, 1876–1891, [https://doi.org/10.1890/11-](https://doi.org/10.1890/11-1785.1)
424 1785.1, 2012.
- 425 Mekonnen, Z. A., Riley, W. J., Randerson, J. T., Grant, R. F., and Rogers, B. M.: Expansion of high-latitude deciduous
426 forests driven by interactions between climate warming and fire, *Nat. Plants*, 5, 952–958,
427 <https://doi.org/10.1038/s41477-019-0495-6>, 2019.
- 428 Mollicone, D., Eva, H. D., and Achard, F.: Human role in Russian wildfires, *Nature*, 440, 436–437,
429 <https://doi.org/10.1038/440436a>, 2006.
- 430 Montesano, P. M., Frost, M., Li, J., Carroll, M., Neigh, C. S. R., Macander, M. J., Sexton, J. O., & Frost, G. V.: A
431 shift in transitional forests of the North American boreal will persist through 2100, *Nature Communications: Earth*
432 *and Environment*, 5, 1, <https://doi.org/10.1038/s43247-024-01454-z>, 2024.
- 433 Neigh, C. S. R., Tucker, C. J., and Townshend, J. R. G.: North American vegetation dynamics observed with multi-
434 resolution satellite data, *Remote Sens. Environ.*, 112, 1749–1772, <https://doi.org/10.1016/j.rse.2007.08.018>, 2008.
- 435 Neigh, C. S. R., Nelson, R. F., Ranson, K. J., Margolis, H. A., Montesano, P. M., Sun, G., and Goetz, S. J.: Taking
436 stock of circumboreal forest carbon with ground measurements, airborne and spaceborne LiDAR, *Remote Sens.*
437 *Environ.*, 137, 274–287, <https://doi.org/10.1016/j.rse.2013.06.019>, 2013.
- 438 Neigh, C., Montesano, P. M., Sexton, J. O., Wooten, M., Wagner, W., Feng, M., Carvalhais, N., Calle, L., & Carroll,
439 M. L.: Russian forests show strong potential for young forest growth, *Nature Communications: Earth and Environment*,
440 6, 1, <https://doi.org/10.1038/s43247-025-02006-9>, 2025.
- 441 Norby, R. J., and Zak, D. R.: Ecological lessons from Free-Air CO₂ Enrichment (FACE) experiments, *Annu. Rev.*
442 *Ecol. Evol. Syst.*, 42, 181–203, <https://doi.org/10.1146/annurev-ecolsys-102209-144647>, 2011.



- 443 Odum, E. P.: The strategy of ecosystem development, *Science*, 164, 262–270,
444 <https://doi.org/10.1126/science.164.3877.262>, 1969.
- 445 Pan, Y., Birdsey, R. A., Fang, J., Houghton, R., Kauppi, P. E., Kurz, W. A., and Phillips, O. L.: A large and persistent
446 carbon sink in the world's forests, *Science*, 333, 988–993, <https://doi.org/10.1126/science.1201609>, 2011.
- 447 Piao, S., Wang, X., Ciais, P., Zhu, B., Wang, T., and Liu, J.: Characteristics, drivers and feedbacks of global greening,
448 *Nat. Rev. Earth Environ.*, 1, 14–27, <https://doi.org/10.1038/s43017-019-0001-x>, 2020.
- 449 Randerson, J. T., Liu, H., Flanner, M. G., Chambers, S. D., Jin, Y., Hess, P. G., and Rasch, P. J.: The impact of boreal
450 forest fire on climate warming, *Science*, 314, 1130–1132, <https://doi.org/10.1126/science.1132075>, 2006.
- 451 Rees, W. G., Stammer, F. M., Danks, F. S., and Vitebsky, P.: Is subarctic forest advance able to keep pace with
452 climate change?, *Glob. Change Biol.*, 26, 3965–3977, <https://doi.org/10.1111/gcb.15181>, 2020.
- 453 Rotbarth, R., Walker, X. J., Mack, M. C., Goetz, S. J., Johnstone, J. F., and Miller, S. N.: Northern expansion is not
454 compensating for southern declines in North American boreal forests, *Nature Communications*, 14, 3373,
455 <https://doi.org/10.1038/s41467-023-39128-8>, 2023.
- 456 Sato, H., Kobayashi, H., Iwahana, G., and Ohta, T.: Endurance of larch forest ecosystems in eastern Siberia under
457 warming trends, *Ecol. Evol.*, 6, 5690–5704, <https://doi.org/10.1002/ece3.2264>, 2016.
- 458 Scheffer, M., Hirota, M., Holmgren, M., van Nes, E. H., and Chapin, F. S.: Thresholds for boreal biome transitions,
459 *Proc. Natl. Acad. Sci. USA*, 109, 21384–21389, <https://doi.org/10.1073/pnas.1219844110>, 2012.
- 460 Schuur, E. A. G., Abbott, B. W., Bowden, W. B., Brovkin, V., Camill, P., Davidson, E. A., and Hayes, D. J.: Climate
461 change and the permafrost carbon feedback, *Nature*, 520, 171–179, <https://doi.org/10.1038/nature14338>, 2015.
- 462 Sexton, J. O., Noojipady, P., Song, X.-P., Feng, M., Song, D. X., Kim, D. H., and Hansen, M. C.: Global, 30-m
463 resolution continuous fields of tree cover: Landsat-based rescaling of MODIS vegetation continuous fields with
464 LiDAR-based estimates of error, *Int. J. Digit. Earth*, 6, 427–448, <https://doi.org/10.1080/17538947.2013.786146>,
465 2013.
- 466 Walker, X. J., Rogers, B. M., Baltzer, J. L., Baltzer, B., Barrett, M., Bourgeau-Chavez, L., and Mack, M. C.: Increasing
467 wildfires threaten historic carbon sink of boreal forest soils, *Nature*, 572, 520–523, <https://doi.org/10.1038/s41586-019-1474-y>, 2019.
- 469 UNFCCC: Report of the Conference of the Parties on its Seventh Session, held at Marrakesh from 29 October to 10
470 November 2001, Addendum Part Two, United Nations Framework Convention on Climate Change, 2002
- 471 Xi, Y., Zhang, W., Wei, F., Fang, Z., & Fensholt, R.: Boreal tree species diversity increases with global warming but
472 is reversed by extremes, *Nature Plants*, <https://doi.org/10.1038/s41477-024-01794-w>, 2024.
- 473 Yan, Y., Piao, S., Hammond, W. M., Chen, A., Hong, S., Xu, H., Munson, S. M., Myneni, R. B., & Allen, C. D.:
474 Climate-induced tree-mortality pulses are obscured by broad-scale and long-term greening, *Nature Ecology and*
475 *Evolution*, <https://doi.org/10.1038/s41559-024-02372-1>, 2024.



476 Zhu, Z., Piao, S., Myneni, R. B., Huang, M., Zeng, Z., Canadell, J. G., and Ciais, P.: Greening of the Earth and its
477 drivers, *Nat. Clim. Change*, 6, 791–795, <https://doi.org/10.1038/nclimate3004>, 2016.

478